Desalination and Water Treatment
www.deswater.com

doi: 10.1080/19443994.2016.1149890

57 (2016) 25256–25266
November

Taylor & Francis
Taylor & Francis Group

Optimization of reactive black 5 degradation using hydrothermally synthesized NiO/TiO_2 nanocomposite under natural sunlight irradiation

K. Salehi[a], B. Shahmoradi[b,*], A. Bahmani[c], M. Pirsaheb[d], H.P. Shivaraju[e]

[a]*Faculty of Health, Department of Environmental Health Engineering, Kurdistan University of Medical Sciences, Sanandaj, Iran, email: kamalsalehi1366@gmail.com*
[b]*Environmental Health Research Center, Kurdistan University of Medical Sciences, Sanandaj, Iran, Tel. +98 87 31827426; Fax: +98 87 33625131; email: bshahmorady@gmail.com*
[c]*Department of Health Education, Shahid Sadoughi University of Medical Sciences and Health Services, Yazd, Iran, email: a_bahmani59@yahoo.com*
[d]*Research Center for Environmental Determinants of Health (RCEDH), Kermanshah University of Medical Sciences, Kermanshah, Iran, email: mpirsaheb@yahoo.com*
[e]*Department of Environmental Science, School of Life Science, J.S.S. University, Shivarathreshwara Nagara, Mysore 570015, India, email: shivarajuenvi@gmail.com*

Received 25 August 2015; Accepted 30 January 2016

ABSTRACT

In this study, the photocatalytic degradation of reactive black 5 using NiO/TiO_2 nanocomposite as catalyst was optimized based on response surface methodology (RSM). NiO/TiO_2 nanocomposite was fabricated through hydrothermal technique (P = autogenous, T = 150˚C). The nanocomposite fabricated was characterized using powder X-ray diffraction, scanning electron microscopy, UV–vis spectrophotometer, and Fourier transmission infrared spectroscopy. The central composite design (CCD) was applied for the experimental design and process optimization. The optimization studies were carried out by changing initial pH, catalyst dosage, dye concentration, and contact time. The high regression coefficient ($R^2 = 0.9460$, $R_{adj} = 0.9040$) between the variables and the response indicated excellent estimation of experimental data by quadratic model. The optimum catalyst dose, pH, dye concentration, and contact time were found to be 2 g/l, 5, 40 mg/l, and 150 min, respectively, and under the optimal values of process parameters, the dye degradation performance of 86.1% was achieved. Based on the data of present study, it is concluded that CCD and RSM could be employed to model dye degradation parameters using NiO/TiO_2 nanocomposite while optimizing and minimizing the number of experiments required.

Keywords: Optimization; Photocatalysis; Modeling; NiO/TiO_2 nanocomposite; Dye

1. Introduction

Currently, environmental pollution has increased more and more public concern. For example, wastewater containing dyes resulting from textiles, leather, paper, and plastics industries is generally high in both color and organic content [1,2]. One of the largest class of synthetic dyes used in industries is azo dyes. It has been estimated that approximately 70% of all dyes used in the colored industry are azo dyes [3]. These dyes are

---

*Corresponding author.

characterized by the presence of one or more azo bonds (–N=N–) conjugated with aromatic systems, which may also take sulfonic acid groups [4]. Synthetic origin and complex aromatic structure of the dyes make them resistant against microbial biodegradation, therefore, they are not easily degraded through traditional wastewater treatment processes. Hence, their elimination from the effluent is very essential to prevent the entry of colored hazardous materials to nature [5,6]. Some traditional methods such as adsorption [7], nanofiltration membrane [8], electrocoagulation [9], and photodegradation [10,11] have been employed for the treatment of azo dyes containing wastewater. Nevertheless, these methods suffer from some defects such as sludge generation, high treatment costs, adsorbent regeneration, and membrane fouling [3,12]. In the recent years, the application of TiO_2 using solar energy for degradation reactions has attracted the researchers' interest [13]. However, the practical applications of TiO_2, as a green technology, are limited by the inability to utilize visible light, insufficient quantum efficiency, or the possible photodegradation of the catalyst [14]; TiO_2 can only absorb a small portion (3–5%) of solar spectrum in the UV region, resulting in low-photocatalytic efficiency [15,16]. Designing novel catalysts to meet these technical needs is still a challenge [17]. For improving the activity of TiO_2 toward environmental applications, the absorption of light in the visible light spectrum must be enhanced [18]. Therefore, many methods have been used to improve photocatalytic efficiency of TiO_2-based photocatalysts into the visible light region, including doping TiO_2 materials with other impurities such as metals or non-metal elements, photosensitization, and composite semiconductors [19,20]. Moreover, conventional designing experiments are time consuming and require more energy to obtain photodegradation results. Response surface methodology (RSM) is a powerful experiment design tool used widely to design, optimize, and evaluate the performance of multivariable systems. In addition, it gives a complete interaction effects of all of the parameters influencing the process [21,22]. The main advantages of RSM lie in the fact that this method builds models quickly, is less time consuming than the classical methods, cost-effective, and more accurate in an optimization design [23,24].

Thus, the aim of this study was to synthesize NiO/TiO_2 nanocomposite and to investigate the photocatalytic degradation of reactive black 5 (RB5), a model azo dye, in the presence of natural sunlight. NiO/TiO_2 nanocomposite was synthesized via hydrothermal method and RSM was used for the experimental design and optimization of RB5 degradation.

2. Materials and methods

2.1. Materials

Reagent grade TiO_2, NiO, triethylamine and HCl were purchased from Merck, Germany. Water type-one and double distilled water were produced by a TKA Smart 2 ultrapure water production system (Thermo Electron LED GmbH, Germany). RB5 (Alvan Sabet Co., Iran) was used as a model pollutant from textile industry. Table 1 shows the chemical structure and some characteristics of this dye.

2.2. Experimental

NiO/TiO_2 nanocomposite was fabricated under mild hydrothermal conditions ($T = 150$°C, P = autogenous, $t = 12$ h). Three moles of ZnO, 1 mol of nickel oxide, and 10 ml of 1 mol HCl were added into a Teflon liner ($V_{\text{fill}} = 10$ mL). At the same time, a fixed volume (1 ml) of triethylamine was added to the above-mentioned mixture and it was stirred vigorously for a few minutes. Later, the Teflon liner was placed inside a General Purpose autoclave. Then, the assembled autoclave was kept in an oven with a temperature programmer-controller for 12 h. The temperature was kept at 150°C. After the experimental run, the autoclave was quenched to the room temperature. The product in the Teflon liner was then transferred to a clean beaker, washed with double distilled water several times, and then allowed to settle down. The surplus solution was removed using a syringe. Then, the remnant was allowed to dry naturally at room temperature. The dried particles were subjected to systematic characterization and photocatalytic studies.

3. Results and discussion

3.1. Characterization of NiO/TiO_2 nanocomposites

3.1.1. Powder XRD

The crystal structure of NiO/TiO_2 nanocomposite was evaluated using Powder X-ray diffraction (XRD). The XRD plot was taken in the angular range of $2\theta = 5°–110°$. The XRD plot of NiO/TiO_2 was checked and assessed with reagent grade TiO_2 and NiO using Match software (CRYSTAL IMPACT, Germany). As Fig. 1 indicates, mixed phases of NiO and TiO_2 were observed in the XRD pattern. However, the dominated phase is TiO_2 (anatase phase). Moreover, the peaks of crystal were slightly displaced, which could be attributed to the effect of NiO on the TiO_2 lattice.

Table 1
The chemical properties of RB5

Molecular structure	Molecular formula	Molecular weight (g/mol)	λ_{max} (nm)
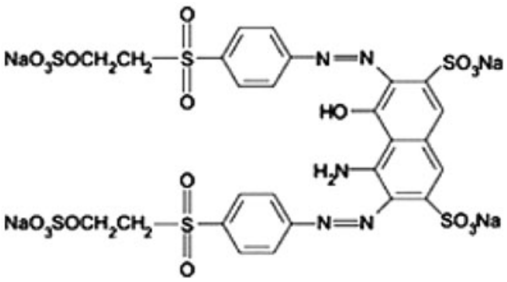	$C_{26}H_{21}N_5Na_4O_{19}S_6$	992.82	597

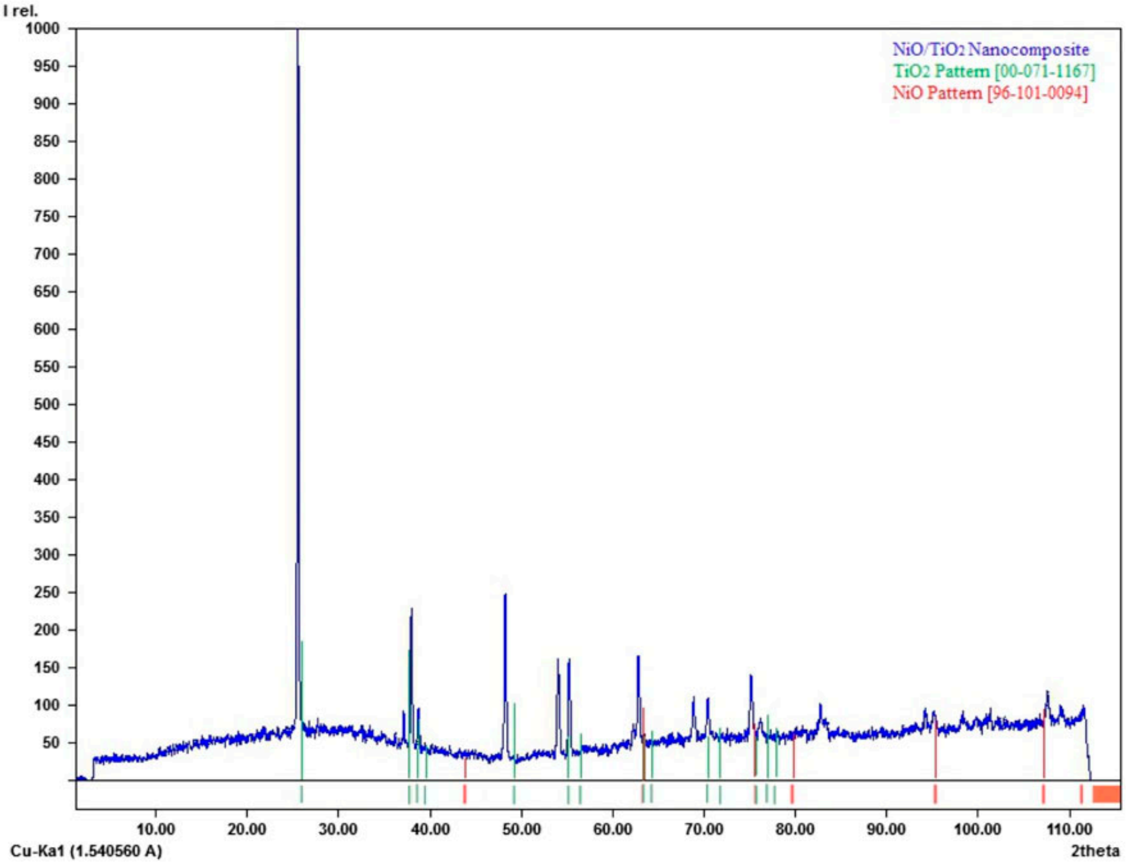

Fig. 1. Powder XRD plot of NiO/TiO_2 nanocomposite.

3.1.2. Scanning electron microscopy

The morphology of NiO/TiO_2 nanocomposite was investigated using Scanning Electron Microscopy (SEM) (Fig. 2). It is evident that the nanocomposite has a spherical structure with no agglomeration, which could be contributed to the effect of surface modifier applied [25]. Moreover, most of the particles are homogeneous, having uniform structure with different size distribution.

3.1.3. FT-IR analysis

Fig. 3 shows the FT-IR spectrum of NiO/TiO_2 nanocomposite. In order to assign the FT-IR spectrum,

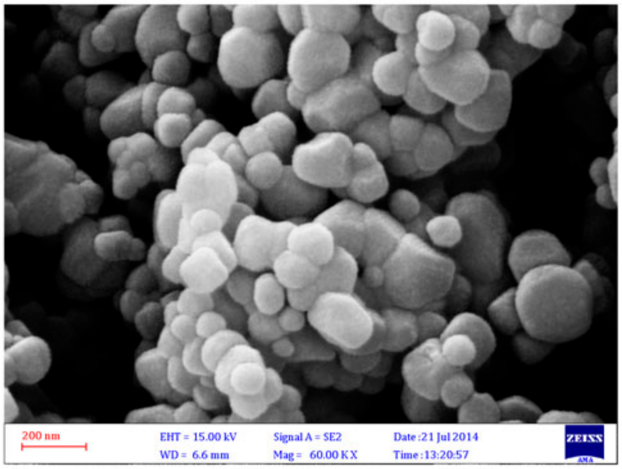

Fig. 2. SEM image of NiO/TiO_2 nanocomposite.

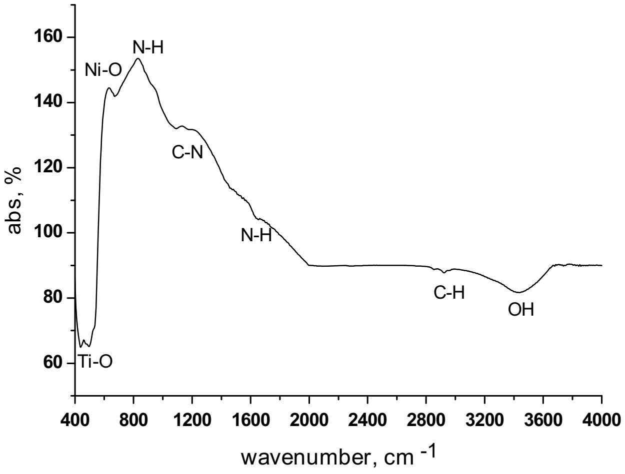

Fig. 3. FT-IR Spectrum of NiO/TiO_2 nanocomposite.

the absorption peaks were compared with the standard pattern [26]. The spectrum was recorded in the wavelength range 400–4,000 cm^{-1}. The peaks around 400–500, 750, and 850 cm^{-1} are attributed to the Ti–O bond in the TiO_2 lattice, the Ni–O bond stretching, and N–H group in surface modifier, respectively. The sharp peak with medium intensity at 1,200 cm^{-1} is assigned to the C–N group. The bands at 1,600 and 2,900 cm^{-1} correspond to N–H and C–H bond stretching, respectively. In addition, the broadband at 3,400 cm^{-1} was observed. It indicates the presence of OH groups absorbed by the sample from the atmosphere.

3.1.4. Bandgap energy of NiO/TiO_2 nanocomposite

One of the drawbacks of using TiO_2 in photocatalytic applications lies in its large bandgap, E_g, which limits the spectrum of photons that can create electron−hole pairs to participate in oxidation or reduction reactions to the UV and corresponds to only 4% of the incident solar energy [27]. The E_g of NiO and TiO_2 are 3.86 and 3.20 eV, respectively [28]. UV–vis spectrophotometer was used for determining the effect of adding NiO on the optical properties of TiO_2. As Fig. 4 indicates, the absorption edge of NiO/TiO_2 nanocomposite was decreased. This red shift can be attributed to the charge transfer transitions between the metal ion *d* electrons and the conduction or valence band of TiO_2 [29].

3.2. Photocatalytic degradation of RB5

The dye degradation experiments were carried out by mixing different amounts of NiO/TiO_2 nanocomposite (0.5–2.5 g/l) for RB5 in a beaker containing 200 ml of a dye solution (40–800 mg/l) and at various pH (3–11). Before exposing the sample into the sunlight illumination, the solution was kept in darkness under continuous shaking for 30 min in order to reach adsorption/desorption equilibrium. However, no adsorption was observed after keeping the solution in darkness. The initial pH of the solution was adjusted before the experiment using 0.1 N NH_3OH or HCl and was controlled using pH meter. Then, solution was irradiated under natural sunlight. The period of the experiment was between 11:30 and 14:30 during the month of June. At specific time intervals, 5 ml of the dye sample was taken out from the system. Each sample was centrifuged for 5 min at 5,000 rpm. The maximum wavelength (λ_{max}) used for the determination of residual concentration of RB5 in the solution

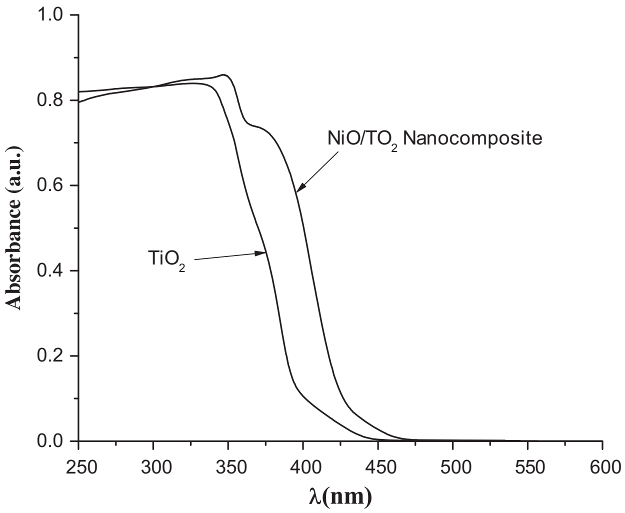

Fig. 4. Bandgap energy of NiO/TiO_2 nanocomposite.

was 618 nm using UV–vis spectrophotometer. The degradation efficiency ($R\%$) was calculated using the following equation:

$$\text{Degradation efficiency}\,(R\%) = (A_0 - A)/A_0 \times 100 \quad (1)$$

where A_0 and A are the dye concentration (mg/l) at time 0 and t respectively in Eq. (1).

3.3. Experimental design and data analysis

In the present study, central composite design (CCD) optimized the degradation of RB5 in the presence of natural sunlight using NiO/TiO_2. The statistical software “Design Expert” (Version 8) was applied for CCD. Independent variables for this investigation were catalyst dosage, pH, contact time, and dye concentration. As a result, the CCD matrices of 31 experiments were designed at 5 levels consisting of 16 factorial points, 8 axial points ($\alpha = 2$), and 7 replicates at the center point (Table 2).

The treatment of the dye degradation process is explained by an empirical quadratic model. A quadratic model, which also includes the linear model, is given as:

$$\eta = b_0 + \sum_{i=1}^{n} b_i x_i + \sum_{i=1}^{n} b_{ii} x_i^2 + \sum_{i=1}^{n-1} \sum_{i=1}^{n} b_{ij} x_i x_j \quad (2)$$

where η is the dye removal performance, b_0 the constant coefficient, b_i the linear coefficient, b_{ii} the quadratic coefficient, b_{ij} the interaction coefficient, and x_i and x_j are the coded values of the variables [5].

3.4. Modeling and optimization of RB5 photodegradation

The experimental results of dye degradation by nanocomposite synthesized were analyzed through RSM to obtain an empirical model. Based on these results, an empirical relationship between the responses and independent variables was achieved for dye degradation expressed by quadratic polynomial equation (Eq. (3)):

$$\begin{aligned} R = {} & (-181.66) + (20.52\,X_1) + (68.61\,X_2) + (0.9973\,X_3) \\ & + (4.327\,X_4) + (-1.318\,X_1X_2) + (-7.08\,X_1X_3) \\ & + (-0.101\,X_1X_4) + (0.0175\,X_2X_3) + (-8.21\,X_1X_4) \\ & + (-1.6297\,X_1^2) + (-15\,X_2^2) + (-3.688\,X_3^2) \\ & + (-0.048504\,X_4^2) \end{aligned} \quad (3)$$

In Eq. (3), R is the response degradation percent, X_1, X_2, X_3, and X_4 are corresponding to independent variables of pH, catalyst dosage (g/l), contact time (min), and dye concentration (mg/l) respectively.

Table 3 presents the results of ANOVA analysis of the quadratic models. ANOVA checks adequacy of the developed model and statistical significance of the regression coefficients [30].

Moreover, in Table 3, the quadratic model F-value of 37.97 implies that the model is significant for the degradation of RB5 and there is only a 0.01% chance that a “model F-value”; this large could occur due to noise. Adequate precision measures the signal to noise ratio and a ratio greater than 4 is generally desirable [3,31]. Therefore, in the quadratic model of RB5 degradation, the ratio of 23.53 indicated an adequate signal. The square of correlation coefficient for responses was computed as the R^2. The goodness of fit of the model was also checked by the multiple correlation coefficient. The R^2 value of 0.9460 for degradation of RB5 using NiO/TiO_2 nanocomposite and corresponding adjusted R^2 0.9040 are close to 1.0 indicating a high correlation between the observed values and the predicted values [12]. Table 4 presents the optimum conditions for maximum efficiency of dye photodegradation.

Fig. 5 shows the relationship between the actual and the predicted values for the degradation of RB5 using NiO/TiO_2 nanocomposite. Actual values and perfected values were measured from the response data for a particular run and the model, respectively. The results showed that the predicated values and the actual values obtained for dye degradation were high. In addition, it was found that the models developed were effectual in taking correlation between nanocomposite type variables and degradation of dye [32,33].

Table 2
Experimental design of photocatalytic degradation of RB5 dye using NiO/TiO2 nanocomposite

Factor	Name	Low actual	Height actual
X_1	pH	3	11
X_2	Catalyst dosage (g/l)	0.5	2.5
X_3	Contact time (min)	60	180
X_4	Dye concentration (mg/l)	40	80

Table 3
ANOVA result of the quadratic model of photocatalytic degradation of RB5 dye using NiO/TiO_2 nanocomposite

Source	Sum of square	DF	Mean square	*F*-value	*p*-value
Model	12,138.79	14	867.04	37.97	<0.0001
X_1	987.44	1	987.44	43.24	<0.0001
X_2	65.95	1	65.95	2.89	<0.0001
X_3	26.21	1	26.21	1.15	0.2999
X_4	835.32	1	835.32	36.58	<0.0001
X_1X_2	27.83	1	27.83	1.22	0.2860
X_1X_3	2.89	1	2.89	0.13	0.7267
X_1X_4	65.61	1	65.61	2.87	0.1065
X_2X_3	1.10	1	1.10	0.048	0.8289
X_2X_4	0.12	1	0.12	5.39	0.9425
X_3X_4	0.950	1	0.95	0.042	0.8454
X_1^2	1,215.31	1	1,215.31	53.21	<0.00001
X_2^2	450.51	1	450.51	19.73	0.0042
X_3^2	247.45	1	247.45	10.48	0.0046
X_4^2	672.76	1	672.76	29.46	<0.0001
Residual	345.60	16	22.48	–	–
Lack of fit	365.08	10	36.51	695.39	<0.0001
Total	12,504	30	–	–	–

Notes: X_1 = pH, X_2 = catalyst dosage, X_3 = contact time, X_4 = dye concentration, $R^2 = 0.9460$, R^2-(adj) = 0.9040.

Table 4
Optimum values of the process parameter for maximum efficiency

Parameter	Optimum value BR5
η (efficiency, %)	0.861
X_1 (pH)	5
X_2 (catalyst dosage, g/l)	2
X_3 (contact time, min)	150
X_4 (concentration dye, mg/l)	40

A suitable graphical method for judging and explaining the systematic departures from the assumption that errors are normally distributed and are independent of each other is the normal probability plot of the residuals. Plot of residual vs. the predicted response is presented in Fig. 6. Based on this plot, the residuals appear to be randomly scattered and all the residual values are within the range of −3 and +3 (values between −3 and +3 being the acceptable limit), thereby validating the model [34,35].

The effect of operating parameters of pH, catalyst dosage, initial dye concentration, and contact time on dye degradation are shown in the response surface graphs in Figs. 6–8. As shown in Fig. 6, degradation efficiency (%) of RB5 dye decreased with an increase in initial solution pH and the maximum degradation efficiency was observed at pH 5.0. This can be explained based on zero point of charge (pH_{zpc}) of TiO_2. The point of pH_{zpc} for TiO_2 nanoparticles is about 6.5 [36]. In acidic solution, TiO_2 surface is positively charged, while it is negatively charged in alkaline solution. RB5 is an anionic dye, which after ionization at acidic pH, has a tendency to be adsorbed onto the TiO_2 surface. As a result, positively charged surface of TiO_2 enhanced the adsorption of RB5 by the electrostatic attraction, which would increase the degradation of RB5. But, in alkaline medium, the surface of TiO_2 has become negatively charged that leads to the electrostatic repulsion between RB5 and nanocomposite, which results in decreasing the degradation efficiency [4,37].

Fig. 7 represents the effects of catalyst dosage and contact time on the degradation of RB5 by NiO/TiO_2 nanocomposite at an initial dye concentration of 30 mg/l and pH of 5. As depicted in Fig. 6, the degradation efficiency increased as the NiO/TiO_2 nanocomposite ratio increased from 0.5 to 2 g/l and then decreased as the ratio increased from 2 to the highest value of 2.5. This can be explained on the basis that the increase in catalyst loading is accompanied by an increase in the number of active sites on the NiO/TiO_2 surface, which increase the number of hydroxyl and superoxide radicals. However, when the catalyst loading exceeded the limiting value, due to decrease in sunlight penetration into the solution, causes a decrease in the RB5 degradation rate. Moreover, at high photocatalyst dosage the photocatalyst surface reduced due to the agglomeration [38,39].

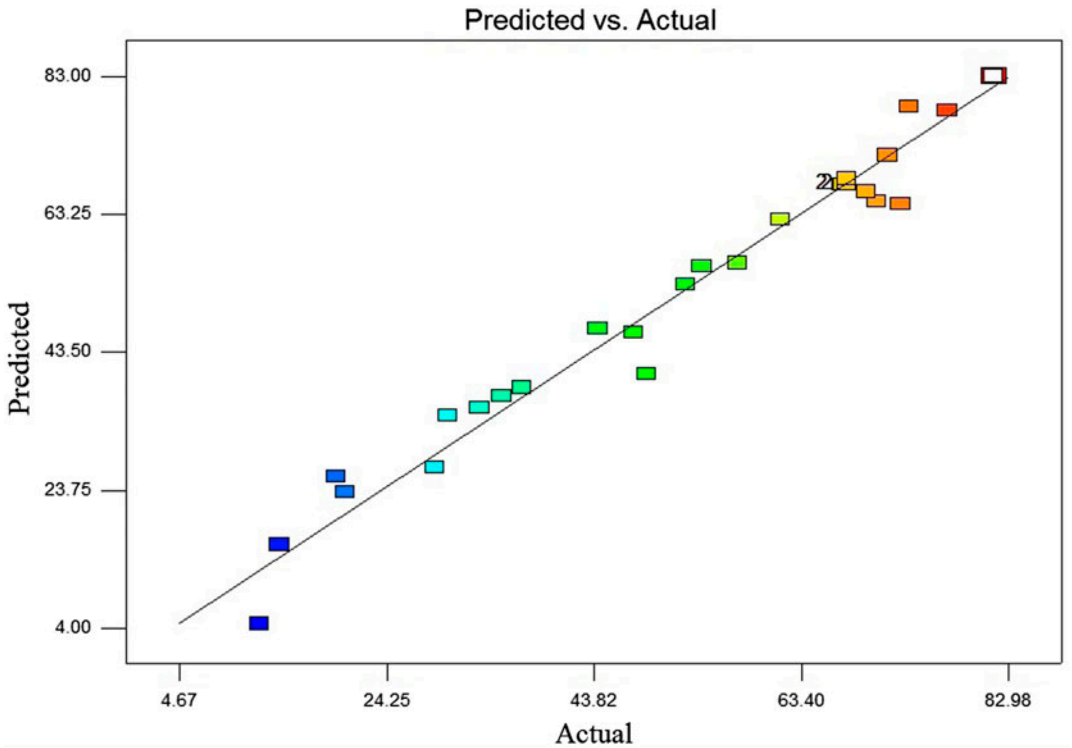

Fig. 5. Plot of the predicted vs. the experimental degradation efficiency.

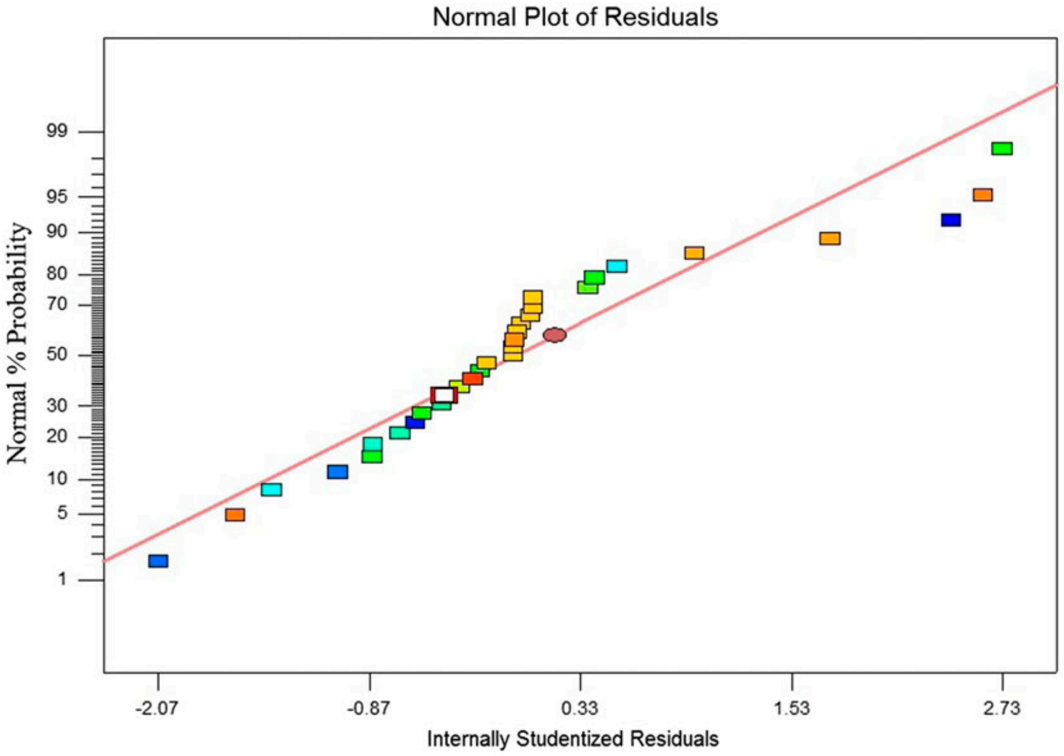

Fig. 6. Plot of the normal probability of the raw residuals.

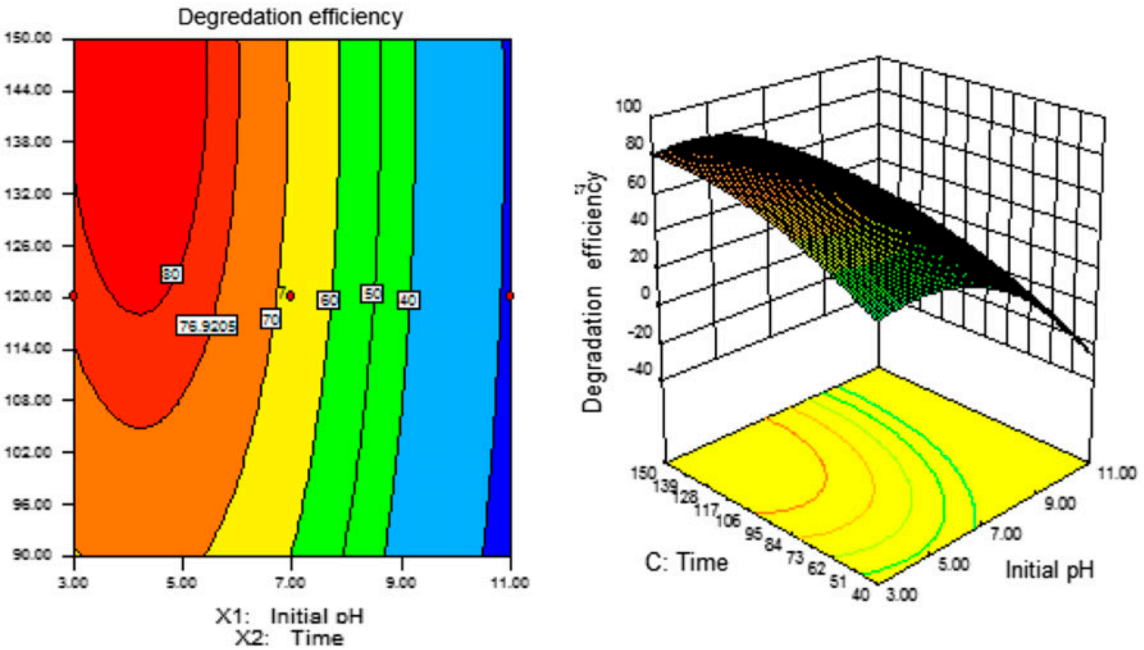

Fig. 7. The response surface plot and corresponding counter plot of RB5 as the function of initial pH and reaction time (min). NiO/TiO_2 = 1.5 g/l, initial dye concentration = 40 mg/l.

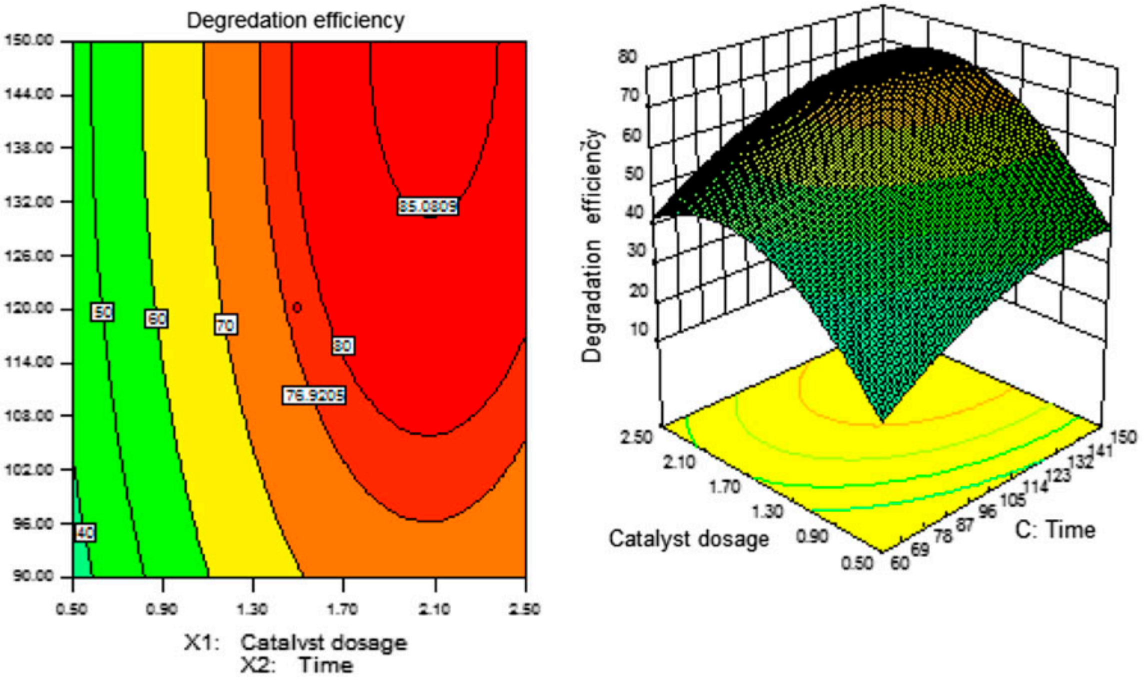

Fig. 8. The response surface plot and counter plot of RB5 as the function of initial catalyst dosage (g/l), contact time (min), Initial pH 5, and initial dye concentration = 40 (mg/l).

The effect of the initial dye concentration on the degradation efficiency is shown in Fig. 9 at a nanocomposite ratio of 1.5 and initial pH of 5. Fig. 9 shows that increasing initial dye concentration from 40 to 80 mg/l results in decreasing degradation efficiency. At high dye concentrations, the formation

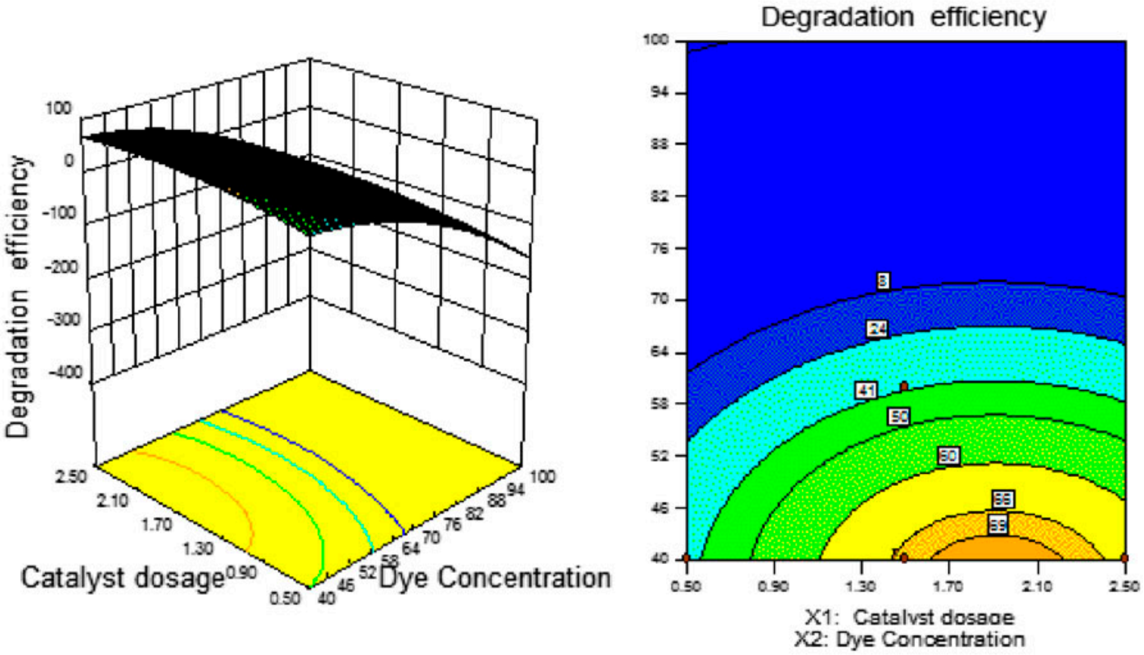

Fig. 9. The response surface plot and counter plot of RB5 degradation as the function of initial dye concentration, pH, initial catalyst dosage = 1.5 g/l, and reaction time = 150 min.

reactive oxygen species on the photocatalyst surface is reduced. In addition, as the concentration of solution increases the path length of photon entering into the dye solution decreased, thus, only fewer photons reached the catalyst surface. Hence, the absorption of photons by the catalyst decreases, and consequently, the degradation efficiency decreases [40,41].

4. Conclusion

In this investigation, the photocatalytic degradation of a simulated dyestuff effluent, containing RB5 as colorant, was studied and the effects of the operating variables including initial dye concentration, NiO/TiO_2 dosage, pH, and time on degradation efficiency were investigated using RSM method. Results of ANOVA analysis indicated a high coefficient of determination value ($R^2 = 0.9460$, $R_{adj} = 0.9040$), therefore ensuring a satisfactory adjustment of the quadratic model with the experimental data. In addition, an optimum condition for the degradation process using RSM was achieved at dye concentration of 40 mg/l, initial pH value of 5, catalyst dosage 2 g/l, and contact time of 150 min for RB5. Based on the results obtained, it is concluded that the RSM is one of the suitable methods to optimize the best operating conditions to maximize the dye removal.

Acknowledgment

The authors are thankful for the financial support provided by the Kurdistan University of Medical Sciences, Sanandaj, Iran.

References

[1] H. Tajizadegan, M. Jafari, M. Rashidzadeh, A. Saffar-Teluri, A high activity adsorbent of ZnO–Al_2O_3 nanocomposite particles: Synthesis, characterization and dye removal efficiency, Appl. Surf. Sci. 276 (2013) 317–322.

[2] O. Iglesias, M.F. de Dios, E. Rosales, M. Pazos, M. Sanromán, Optimisation of decolourisation and degradation of Reactive Black 5 dye under electro-Fenton process using Fe alginate gel beads, Environ. Sci. Pollut. Res. 20 (2013) 2172–2183.

[3] H.-Y. Xu, W.-C. Liu, J. Shi, H. Zhaoand, S.-Y. Qi, Photocatalytic discoloration of Methyl Orange by anatase/schorl composite: Optimization using response surface method, Environ. Sci. Pollut. Res. 21 (2014) 1582–1591.

[4] J. Sun, L. Qiao, S. Sunand, G. Wang, Photocatalytic degradation of Orange G on nitrogen-doped TiO_2 catalysts under visible light and sunlight irradiation, J. Hazard. Mater. 155 (2008) 312–319.

[5] M. Kousha, E. Daneshvar, H. Dopeikar, D. Taghavi, A. Bhatnagar, Box-Behnken design optimization of Acid Black 1 dye biosorption by different brown macroalgae, Chem. Eng. J. 179 (2012) 158–168.

[6] M. Vaez, A. Zarringhalam Moghaddam, S. Alijani, Optimization and modeling of photocatalytic degradation of azo dye using a response surface methodology

(RSM) based on the central composite design with immobilized titania nanoparticles, Ind. Eng. Chem. Res. 51 (2012) 4199–4207.

[7] T.K. Saha, N.C. Bhoumik, S. Karmaker, M.G. Ahmed, H. Ichikawa, Y. Fukumori, Adsorption characteristics of reactive black 5 from aqueous solution onto chitosan, Clean—Soil Air Water 39 (2011) 984–993.

[8] T.N. Patel, K. Nath, Separation of ternary sodium chloride/Reactive Black-5 aqueous solutions using two different modules in a nanofiltration pilot plant, Int. J. Environ. Sci. Technol. 11 (2014) 1237–1248.

[9] İ.A. Şengil, M. Özacar, The decolorization of C.I. Reactive Black 5 in aqueous solution by electrocoagulation using sacrificial iron electrodes, J. Hazard. Mater. 161 (2009) 1369–1376.

[10] B. Shahmoradi, A. Maleki, K. Byrappa, Photocatalytic degradation of Amaranth and Brilliant Blue FCF dyes using *in situ* modified tungsten doped TiO_2 hybrid nanoparticles, Catal. Sci. Technol. 1 (2011) 1216–1223.

[11] S. Laohaprapanon, J. Matahum, L. Tayo, S.-J. You, Photodegradation of Reactive Black 5 in a ZnO/UV slurry membrane reactor, J. Taiwan Inst. Chem. Eng. 49 (2015) 136–141.

[12] A. Khataee, M. Fathinia, S. Aber, M. Zarei, Optimization of photocatalytic treatment of dye solution on supported TiO_2 nanoparticles by central composite design: Intermediates identification, J. Hazard. Mater. 181 (2010) 886–897.

[13] B. Shahmoradi, M. Negahdary, A. Maleki, Photodegradation of methylene blue using surface modified manganese doped TiO_2 nanoparticles, Environ. Eng. Sci. 29 (2012) 1032–1037.

[14] N. Zhang, Y. Zhang, Y.-J. Xu, Recent progress on graphene-based photocatalysts: Current status and future perspectives, Nanoscale 4 (2012) 5792–5813.

[15] G.S. Pozan, A. Kambur, Significant enhancement of photocatalytic activity over bifunctional ZnO–TiO_2 catalysts for 4-chlorophenol degradation, Chemosphere 105 (2014) 152–159.

[16] M. Safari, R. Talebi, M.H. Rostami, M. Nikazar, M.J. Dadvar, Synthesis of iron-doped TiO_2 for degradation of reactive Orange16, J. Environ. Health Sci. Eng. 12 (2014) 19, doi: 10.1186/2052-336X-12-19.

[17] N. Zhang, M.-Q. Yang, S. Liu, Y. Sun, Y.-J. Xu, Waltzing with the versatile platform of graphene to synthesize composite photocatalysts, Chem. Rev. 115(18) (2015) 10307–10377, doi: 10.1021/acs.chemrev.5b00267.

[18] G.C. Collazzo, E.L. Foletto, S.L. Jahn, M.A. Villetti, Degradation of Direct Black 38 dye under visible light and sunlight irradiation by N-doped anatase TiO_2 as photocatalyst, J. Environ. Manage. 98 (2012) 107–111.

[19] B. Shahmoradi, I.A. Ibrahim, K. Namratha, N. Sakamoto, S. Ananda, R. Somashekar, K. Byrappa, Surface modification of indium doped ZnO hybrid nanoparticles with *n*-butylamine, Int. J. Chem. Eng. Res. 2 (2010) 107–117.

[20] M.-I. Dai, L.-X. Guan, F. Li, M.-M. Yao, Titanium dioxide composite films for enhanced photocatalytic activity, Ceram. Int. 40 (2014) 7651–7655.

[21] Z. Shaykhi, A. Zinatizadeh, Statistical modeling of photocatalytic degradation of synthetic amoxicillin wastewater (SAW) in an immobilized TiO_2 photocatalytic reactor using response surface methodology (RSM), J. Taiwan Inst. Chem. Eng. 45 (2014) 1717–1726.

[22] B.K. Körbahti, M. Rauf, Application of response surface analysis to the photolytic degradation of Basic Red 2 dye, Chem. Eng. J. 138 (2008) 166–171.

[23] K. Ravikumar, K. Pakshirajan, T. Swaminathan, K. Balu, Optimization of batch process parameters using response surface methodology for dye removal by a novel adsorbent, Chem. Eng. J. 105 (2005) 131–138.

[24] A. Witek-Krowiak, K. Chojnacka, D. Podstawczyk, A. Dawiec, K. Pokomeda, Application of response surface methodology and artificial neural network methods in modelling and optimization of biosorption process, Bioresour. Technol. 160 (2014) 150–160.

[25] K. Salehi, H. Daraei, P. Teymouri, A. Maleki, Hydrothermal synthesis of surface-modified copper oxide-doped zinc oxide nanoparticles for degradation of acid black 1: Modeling and optimization by response surface methodology, J. Adv. Environ. Health Res. 2 (2014) 101–109.

[26] D.L. Pavia, G.M. Lampman, G.S. Kriz, Infrared spectroscopy, in: Introduction to Spectroscopy, third ed., Thomson Learning, USA, 2001, pp. 13–101.

[27] C. Dette, M.A. Pé rez-Osorio, C.S. Kley, P. Punke, C.E. Patrick, P. Jacobson, F. Giustino, S.J. Jung, K. Kern, TiO_2 anatase with a bandgap in the visible region, Nano Lett. 14(11) 2014 6533–6538, doi: 10.1021/nl503131s.

[28] J.-Z. Chen, T.-H. Chen, L.-W. Lai, P.-Y. Li, H.-W. Liu, Y.-Y. Hong, D.-S. Liu, Preparation and characterization of surface photocatalytic activity with NiO/TiO_2 nanocomposite structure, Materials 8 (2015) 4273–4286.

[29] L. Ganesh, A.K. Gupta, P.P. Kumar, P.S.C. Sekhar, K. Radha, G. Padmanabham, G. Sundararajan, Preparation and characterization of Ni-doped TiO_2 materials for photocurrent and photocatalytic applications, Sci. World J. 2012 (2012) 127326, doi: 10.1100/2012/127326.

[30] K. Sinha, P.D. Saha, S. Datta, Response surface optimization and artificial neural network modeling of microwave assisted natural dye extraction from pomegranate rind, Ind. Crops Prod. 37 (2012) 408–414.

[31] M. Kousha, E. Daneshvar, M. Sohrabi, N. Koutahzadeh, A. Khataee, Optimization of CI Acid Black 1 biosorption by *Cystoseira indica* and *Gracilaria persica* biomasses from aqueous solutions, Int. Biodeterior. Biodegrad. 67 (2012) 56–63.

[32] A. Buntić, M. Pavlović, K. Mihajlovski, M. Randjelović, N. Rajić, D. Antonović, S. Šiler-Marinković, S. Dimitrijević-Branković, Removal of a cationic dye from aqueous solution by microwave activated clinoptilolite—Response surface methodology approach, Water Air Soil Pollut. 225 (2014) 1816, doi: 10.1007/s11270-013-1816-6.

[33] M. Şener, D. Reddy, B. Kayan, Biosorption properties of pretreated sporopollenin biomass for lead(II) and copper(II): Application of response surface methodology, Ecol. Eng. 68 (2014) 200–208.

[34] R. Soltani, A. Rezaee, A. Khataee, M. Safari, Photocatalytic process by immobilized carbon black/ZnO nanocomposite for dye removal from aqueous medium: Optimization by response surface methodology, J. Ind. Eng. Chem. 20 (2014) 1861–1868.

[35] M.S. Roriz, J.F. Osma, J.A. Teixeira, S.R. Couto, Application of response surface methodological approach to optimise Reactive Black 5 decolouration by crude laccase from *Trametes pubescens*, J. Hazard. Mater. 169 (2009) 691–696.

[36] H. Xu, Q. Zhang, W. Yan, W. Chu, L. Zhang, Preparation and characterization of PbO_2 electrodes doped with TiO_2 and its degradation effect on azo dye wastewater, Int. J. Electrochem. Sci. 8 (2013) 5382–5395.

[37] F. Harraz, R. Mohamed, M. Rashad, Y. Wang, W. Sigmund, Magnetic nanocomposite based on titania–silica/cobalt ferrite for photocatalytic degradation of methylene blue dye, Ceram. Int. 40 (2014) 375–384.

[38] M.A. Behnajady, H. Eskandarloo, Preparation of TiO_2 nanoparticles by the sol–gel method under different pH conditions and modeling of photocatalytic activity by artificial neural network, Res. Chem. Intermed. 41 (2015) 2001–2017.

[39] S. Garcia-Segura, S. Dosta, J.M. Guilemany, E. Brillas, Solar photoelectrocatalytic degradation of Acid Orange 7 azo dye using a highly stable TiO_2 photoanode synthesized by atmospheric plasma spray, Appl. Catal. B: Environ. 132–133 (2013) 142–150.

[40] Z. Zhang, Z. Yuan, G. Shi, Y. Fang, L. Liang, H. Ding, L. Jin, Photoelectrocatalytic activity of highly ordered TiO_2 nanotube arrays electrode for azo dye degradation, Environ. Sci. Technol. 41 (2007) 6259–6263.

[41] D. Qu, Z. Qiang, S. Xiao, Q. Liu, Y. Lei, T. Zhou, Degradation of Reactive Black 5 in a submerged photocatalytic membrane distillation reactor with microwave electrodeless lamps as light source, Sep. Purif. Technol. 122 (2014) 54–59.